

PACS 78.40.Ri

Effect of chemical modification of thin C₆₀ fullerene films on the fundamental absorption edge

N.L. Dmitruk¹, O.Yu. Borkovskaya¹, T.S. Havrylenko¹, D.O. Naumenko¹, P. Petrik², V. Meza-Laguna³, E.V. Basiuk (Golovataya-Dzhymbeeva)³

¹*V. Lashkaryov Institute of Semiconductor Physics, NAS of Ukraine, 45, prospect Nauky, 03028 Kyiv, Ukraine*

²*Research Institute for Technical Physics and Materials Science, Budapest 114, P.O. Box 49, H-1525, Hungary*

³*Centro de Ciencias Aplicadas y Desarrollo Tecnológico,*

Universidad Nacional Autónoma de México, Circuito Exterior C. U., 04510 México D.F., Mexico

Abstract. Fullerene C₆₀ films were grown using physical vapor deposition on Si substrates at room temperature. Then chemical modification with cross-linking these films was performed using the reaction with 1,8-octanediamine (DA) or octane-1,8-dithiol (DT). These chemically cross-linked C₆₀ films are capable of stable binding the Ag or Au nanoclusters. Optical properties of the obtained nanostructured hybrid films were investigated by both reflectance spectroscopy and spectral ellipsometry within the spectral range 1.55 to 5.0 eV at various angles of incidence. From the spectral dependences of the extinction coefficient in the region of optical absorption edge, the physical nature of the fundamental allowed direct band-gap transitions between HOMO-LUMO states E_g , the optical absorption edge near the intrinsic transition E_o , and exponential tail of the density-of-states caused by defects have been determined. Influence of chemical modification and decoration of metal nanoparticles on the above mentioned parameters has been analyzed.

Keywords: fullerene C₆₀ films, chemical modification, optical parameters.

Manuscript received 05.03.10; accepted for publication 25.03.10; published online 30.04.10.

1. Introduction

The advancement of modern electronics, especially optoelectronics and photovoltaics, demands new technologies for manufacturing advanced materials.

Various fullerene-based materials, due to their special optical and electronic properties, have a great potential for application in many nanoelectronic devices. In the recent decade, there has been a great interest to modification of C₆₀ fullerene films on various substrates, especially on silicon substrates due to their wide applications in microelectronic industry. Optical properties of thin fullerite films are very dependent on technology of preparation as well as structure of substrate material. For example, it has been shown in [1] that the optical properties of the C₆₀ films are deeply influenced by the nature of substrate (amorphous or crystalline), temperature and deposition rate. Namely,

the larger film deposition rate results in the higher structural and compositional disorder and in the lower value of the optical density.

Modification of C₆₀ fullerene films on various substrates by using special chemical treatment with 1,8-diaminooctane (or octane-1,8-dithiol) that simultaneously react with neighboring fullerene molecules acting as a cross-linking agents changes solubility of fullerene films and influences on their physical and chemical characteristics [2, 3]. In the work [4], fullerene C₆₀ films were exploited as molecular templates for metal cluster superstructure. Chemical bonding of metal nanoparticles to fullerene support reduced considerably the undesirable coalescence effects. Using an aliphatic bifunctional amine or thiol as linker, the immobilized silver and gold nanoparticles have been obtained. The physical properties of C₆₀ films decorated with Ag and Au nanoparticles depend considerably on the interface configuration.

Formation of metal nanoparticles on the surface of C_{60} film covering silicon substrate is of considerable interest as related with: (1) possibility to enhance transmittance of light into semiconductor due to plasmon resonance excitation in nanoparticles; (2) the local electromagnetic field enhancement near the metal surface and penetration of it into semiconductor base with following generation of non-equilibrium electron-hole pairs [5]; (3) the light scattering by large metal nanoparticles [6]; and (4) the enhancement of optical absorption of incident photons due to increase in duration of interaction between near field and semiconductor.

Besides, using a thin absorbing layer between the conducting emitter and photoactive base, one can change the spectral region of solar cell photosensitivity. So, controlling the fundamental absorption spectral region of fullerene thin films on silicon substrate is very important.

In this work, we study the near fundamental absorption edge for five types of pristine and chemically functionalized fullerene C_{60} films on n -Si substrate: 1) pristine fullerene films (C_{60}/Si); 2) 1,8-diaminooctane-cross-linked C_{60} films ($C_{60}-DA/Si$); 3) cross-linked films decorated with Ag nanoparticles ($C_{60}-DT-Ag/Si$); 4) octane-1,8-dithiol-cross-linked C_{60} films ($C_{60}-DT/Si$); 5) cross-linked films decorated with Au nanoparticles ($C_{60}-DT-Au/Si$).

2. Samples and experimental technique

Deposition of fullerene C_{60} films onto Si was performed in a vacuum chamber at pressure of 6.2×10^{-6} Torr, without heating the substrates. The average film thickness obtained was about 80 to 120 nm.

For gas-phase functionalization, the samples (C_{60}/Si) were taken out from the vacuum sublimation chamber and immediately degassed at low vacuum at 120 °C for 30 min using a custom-made Pyrex manifold [7]. Then, 5 mg of 1,8-diaminooctane were added directly to the reactor bottom, avoiding direct contact with the sample. The gas-phase reaction was carried out at a pressure of ca. 1 Torr and temperature of about 150 °C for 2 h, as was described previously [4]. The high derivatization temperature not only facilitates the reaction, but also enables to minimize the amount of diamine and humidity physically adsorbed on the sample ($C_{60}-DA/Si$) surface.

Deposition of Ag nanoparticles on chemically modified C_{60} films (samples $C_{60}-DA-Ag/Si$) was based on the reduction of $AgNO_3$ with citric acid, as described elsewhere [4, 8]. In a typical experiment, the fullerene samples were placed into 10 ml of 2-propanol. Then two solutions, one of 8.5 mg of $AgNO_3$ in 10 ml of 2-propanol and another one of 19.2 mg of citric acid in

10 ml 2-propanol, were simultaneously added dropwise, while the reaction system was vigorously stirred at room temperature for 30 to 60 min. After finishing the deposition process, the samples were washed with 2-propanol, dried and stored under vacuum at room temperature.

Functionalization of C_{60} films with octane-1,8-dithiol was performed by means of the gas-phase reaction at a pressure of ca. 1 Torr and 140 °C ($C_{60}-DT/Si$). Au nanoparticles decoration of modified C_{60} films ($C_{60}-DT-Au/Si$) was carried out as a result of the reducing chemical reaction between $HAuCl_4$ and citric acid solutions in 2-propanol, simultaneously dropped onto C_{60} film surfaces [9].

Morphology and structure of fullerite films were investigated by means of atomic force microscopy (AFM) using Nanoscope IIIA, Digital Instruments USA and of high-resolution transmission electron microscopy (HRTEM), using JEOL 2010, Japan, respectively.

For optical characterization of investigated films, the reflectance spectra were measured within the energy range $h\nu = 1.1-3.1$ eV at variable angles of incidence for p - and s -polarized light. The fullerene layer thickness value and its optical parameters (refractive index n , and extinction coefficient k in the complex refractive index $\tilde{n} = n - ik$) were determined by fitting experimental dependences with theoretical ones, calculated within the framework of one-layer model for pristine or functionalized C_{60} films. To confirm these results, the ellipsometric measurements were performed using a Woollam M2000DI rotating compensator ellipsometer within the spectral range 1.55 to 5.0 eV at the angles of incidence 45°, 60°, 65° and 75°.

The parameters of fullerite films on semiconductor substrates at the fixed wavelength $\lambda = 632.8$ nm, the refraction index (n) and extinction coefficient (k) were estimated using the multi-angle-of-incidence (MAI) ellipsometry with the laser ellipsometer LEF-3M and He-Ne laser as a source of monochromatic light. Measurements of the polarization angles ψ and Δ were carried out at the angles of incidence $\varphi = 45$ to 83°. The angles ψ and Δ were measured using the double-zone method. The optical parameters n and k have been calculated from dependences of the polarization angles ψ and Δ on the incidence angle φ [10].

The determined parameters were used for calculation of the absorption coefficient $\alpha = 4\pi k/\lambda$. The comprehensive analysis of the $\alpha(h\nu)$ spectra using various coordinate systems allowed us to explain the absorption edge and its modification with both chemical polymerization and metal nanoparticles decoration.

3. Results and discussion

It is well known that C_{60} in the solid state is a typical molecular material with weak bonds between molecules. According to AFM data, the thin films of

fullerene C_{60} have granular (cluster or microcrystallite) structure with the average grain diameter of about 50 nm. Chemical modification of C_{60} films with different organic cross-linkers (*diamine*, *dithiol*) resulted in formation of covalently linked hybrid superstructures, capable of strong binding and immobilization of noble metals. However, the grains of modified films became bigger, their RMS-roughness changes weakly (for example, from 1.22 to 1.08 nm [11]). The treatments with DA and DT reduce solubility of C_{60} films in toluene, indicating the transformation of C_{60} into different solid phases of polymeric nature. Chemical cross-linking the C_{60} molecules removes degeneracy of electron energy levels in the initial C_{60} monomers. Ag nanoparticles on the C_{60} -DA-Ag/Si sample present uniform coverage and are about 5 nm in diameter. For octane-1,8-dithiol functionalized films, the Au nanoparticle sizes distribution exhibit a narrow dispersion with the average diameter 3 nm.

However, the additional chemical treatment leads to changes of surface particles in C_{60} cluster film, and position/intensity of absorption peaks and fundamental absorption edge especially.

Spectra of optical constants, n and k , for pristine and functionalized C_{60} films in the wide spectral range 200-1100 nm are shown in Figs 1a and 1b. The main features of $k(h\nu)$ spectrum for C_{60} film are in agreement with the absorption spectra reported in the literature [1, 12, 13]. We observed the characteristic structure with the absorption maxima at 2.5, 3.6, 4.5 and 5.5 eV. Here, the latter three ones correspond to dipole allowed intramolecular transitions identified as $h_g, g_g \rightarrow t_{1u}$, $h_u \rightarrow h_g$ and $h_g, g_y \rightarrow t_{2u}$, respectively, and the absorption range below 3 eV is caused by the solid-state specific absorption. It is seen that the most essential differences between the spectra of optical constants for pristine and functionalized C_{60} films are observed for the k and $\alpha = 4\pi k/\lambda$ values. Therefore, in Fig. 2 spectra of the light absorption coefficient α are shown within the spectral range $h\nu$ from 1.1 to 3.2 eV for these 5 types of investigated fullerene films: pristine C_{60} , functionalized by diamine or dithiol, C_{60} -DA, C_{60} -DT, and fullerite films with the immobilized gold or silver nanoparticles, C_{60} -DT-Au, C_{60} -DA-Ag. The spectral range of $\alpha(h\nu)$ dependences may be separated into four main parts: I – the part of the more intensive increase of α ($h\nu > 2.2$ eV), II – the optical absorption edge ($h\nu$ from 1.8 to 2.1 eV), which may be analyzed using the Tauc model [14], III – the absorption tail caused by the exponentially distributed states extending into gap of the films, which exhibit characteristic exponential (Urbach) form ($h\nu$ from 1.6 to 1.9 eV), and IV – the low energy absorption band caused by the structure defects and/or impurities, in particular by oxygen [15] ($h\nu < 1.6$ eV). The further treatments of these spectra in various coordinates are shown in Figs 3 to 5.

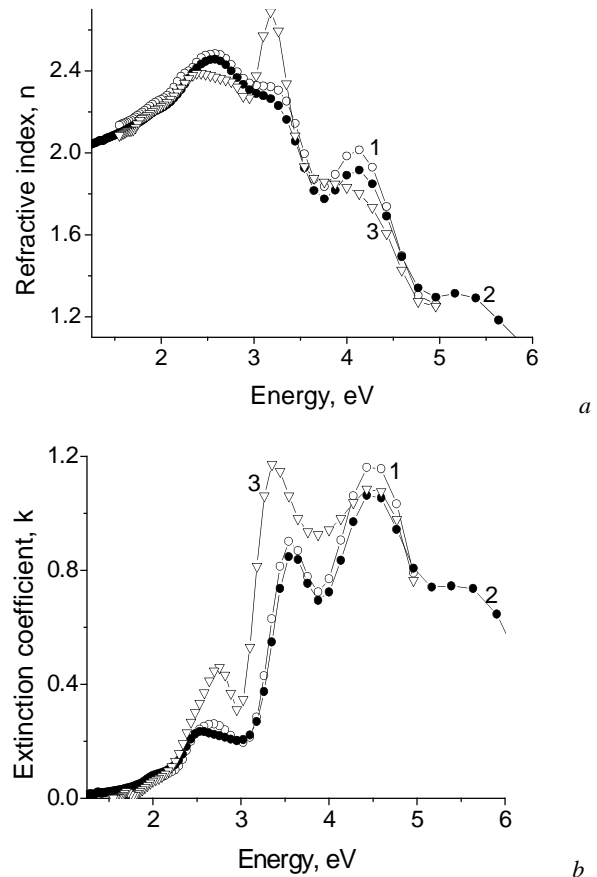


Fig. 1. Spectra of the refractive index (a) and of the extinction coefficient (b) for C_{60} (1), C_{60} -DA (2) and C_{60} -DT-Au (3) films on Si substrate, as determined from the spectral ellipsometric measurements.

The $(\alpha \cdot hv)^2$ vs hv dependences are shown in Figs 3a and 3b. The cutoffs of their linear parts on hv axis determine the direct band gap values for pristine and modified C_{60} films (E_g), which are presented in Table. As it is seen, in the frameworks of experimental errors, the used modifications of C_{60} films do not change their E_g values that coincide with the band gap (2.3 ± 0.1) eV determined in [16] and the mobility gap values of [17]. The alternative interpretation of E_g as intermolecular charge-transfer (CT) exciton energy value [18] is also trustworthy.

Table. The optical absorption edge parameters for pristine and functionalized C_{60} thin films.

Structures	d , nm	E_g , eV	E_o , eV "Tauc gap"	E_U , eV Urbach tail parameter
C_{60}/Si	120	2.36 ± 0.01	1.57 ± 0.01	0.26 ± 0.01
C_{60} -DA/Si	122	2.36 ± 0.01	1.59 ± 0.01	0.25 ± 0.01
C_{60} -DA-Ag/Si	122	2.33 ± 0.01	1.48 ± 0.01	0.16 ± 0.01
C_{60}/Si	80	2.33 ± 0.01	1.68 ± 0.01	–
C_{60} -DT/Si	82	2.35 ± 0.01	1.62 ± 0.01	0.29 ± 0.01
C_{60} -DT-Au/Si	90	2.32 ± 0.01	1.53 ± 0.01	0.23 ± 0.01

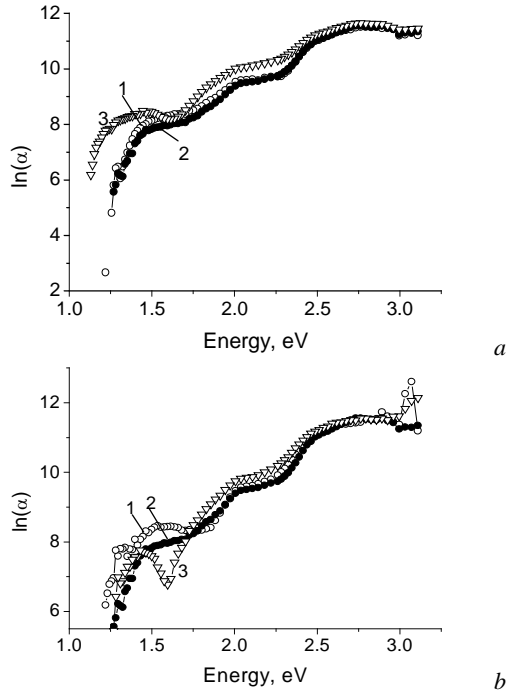


Fig. 2. Semilogarithmic plots of the absorption coefficients spectra for two sets of pristine and modified C_{60} films on Si substrate: (a) – C_{60} (1), C_{60} – DA (2), C_{60} – DA – Ag (3), (b) – C_{60} (1), C_{60} – DT (2), C_{60} – DT – Au (3).

The $(\alpha \cdot hv)^{1/2}$ vs hv dependences, shown in Figs 4a and 4b, allow to determine the optical gap E_o via the Tauc model expression [14] often used for noncrystalline semiconductors

$$\alpha \cdot hv = c(hv - E_o)^2 \quad (1)$$

assuming a parabolic density of states and a constant matrix element of interaction.

It was found that both DA and DT chemical treatments of C_{60} films change E_o value (Table), but the most essential change (decrease of E_o) is observed for chemically modified films decorated with metal nanoparticles (C_{60} -DA-Ag and C_{60} -DT-Au). According to the data of [19], by varying the deposition conditions of C_{60} thin films a continuum of structure types ranging from crystalline to amorphous can be obtained. In the same way, the fundamental optical absorption band gap can be changed from 1.3...1.6 eV for crystalline films to 2.4...2.6 eV for amorphous films. It was shown in [20] that both the extinction coefficient and electron spectrum near the absorption edge are related with differences in the film structure and with suppression of charge-transfer (CT) excitons. The position and intensity of absorption peaks for films grown in argon are changed as compared with the film grown in vacuum [21], without no evidence of chemical changes. Besides, in [21] it was revealed the existence of a mixture of face-centred cubic and hexagonal close-packed phases. All these mean, that intermediate values of optical band gap

may be obtained depending on the degree of film crystallinity, which depends in its turn on the additional chemical treatment by diamine or dithiol.

Fig. 5a and 5b demonstrate the magnified parts of $\ln \alpha$ vs hv dependences for the spectral region III, where they exhibit the characteristic Urbach form:

$$\alpha(hv) = \alpha_0 \exp((hv - E_1)/E_U). \quad (2)$$

Here, α_0 and E_1 are constants, and E_U is the Urbach tail parameter that characterizes the energy extending of the density-of-states into the forbidden gap below the absorption edge (E_o). As it has been shown in [1], the larger the value of E_U , the greater is the compositional, topological or structural disorder of C_{60} films, which depends both on the C_{60} deposition rate and substrate temperature during deposition. So, the known E_U values range from 0.036 eV [15] for C_{60} film, prepared at the substrate (quartz) temperature of 250 °C, to 0.84 eV and even 1.71 eV for the films deposited with the rates 0.14 and 0.44 Å/s, respectively, on the unheated substrates [1]. The E_U values obtained for the investigated films are summarized in Table. It should be noted that the spectral range where the linear parts of dependences shown in Fig. 5 may be considered as those of Urbach type is narrowed in the case of considerable absorption, induced by impurities (oxygen) of region IV. Therefore, the E_U value is omitted for the C_{60} film from the second set of structures.

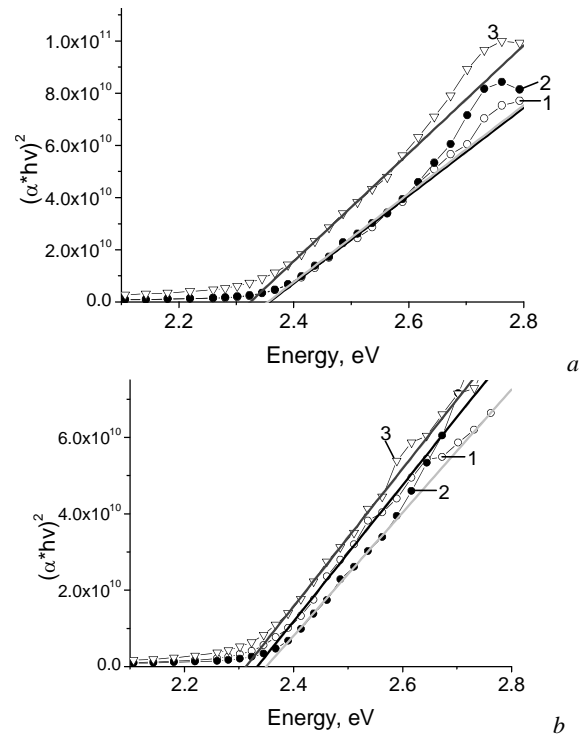


Fig. 3. Spectra of the light absorption coefficients α in coordinates $(\alpha \cdot hv)^2$ vs hv for: (a) – C_{60} (1), C_{60} – DA (2), C_{60} – DA – Ag (3), (b) – C_{60} (1), C_{60} – DT (2), C_{60} – DT – Au (3) films on Si substrate.

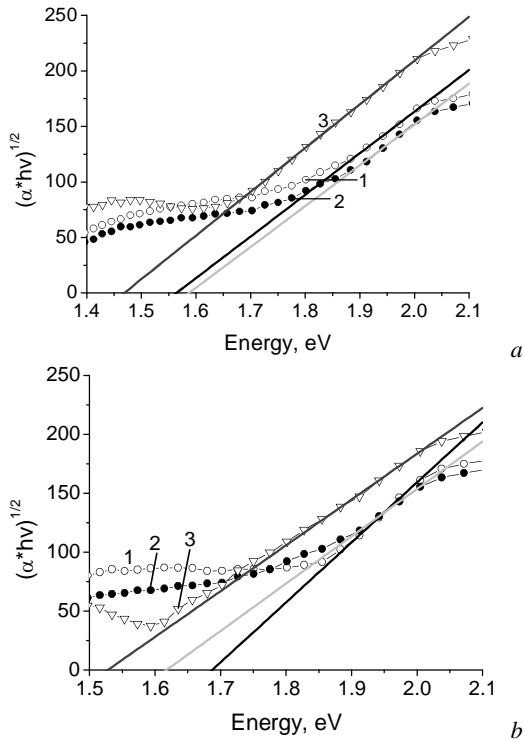


Fig. 4. Spectra of the light absorption coefficients α in coordinates $(\alpha \cdot hv)^{1/2}$ vs hv for: (a) – C_{60} (1), C_{60} – DA (2), C_{60} – DA – Ag (3), (b) – C_{60} (1), C_{60} – DT (2), C_{60} – DT – Au (3) films on Si substrate.

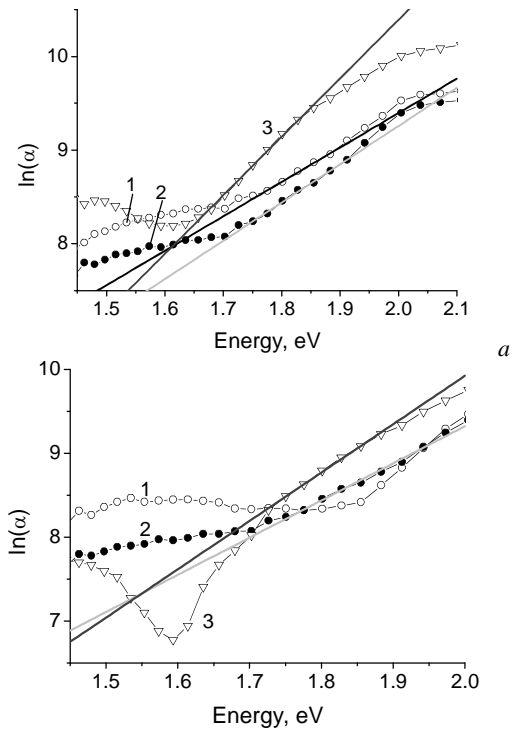


Fig. 5. $\ln \alpha$ vs photon energy dependences for: (a) – C_{60} (1), C_{60} – DA (2), C_{60} – DA – Ag (3), (b) – C_{60} (1), C_{60} – DT (2), C_{60} – DT – Au (3) films on Si substrate.

We observed long-time variations of the optical absorption edge as well, which are associated with a change in the concentration of defects forming shallow tails of the density-of-states.

Thus, the optical parameters of pristine and chemically modified C_{60} films, summarized in Table, demonstrate a certain tendency of their change in consequence of chemical modification with diamine and dithiol, and especially after deposition of the metal (Ag and Au) nanoparticles. These dependences are somewhat apparently weakened due to the one-layer model used for computation of optical parameters for modified C_{60} films. Nevertheless, the determined parameters allow calculating both the absorption and transmittance spectra in these films, which is necessary for the analysis of photoelectric properties of barrier structures including these layers [3, 7]. It should be noted that diamine and dithiol treatments of C_{60} film influence differently on the E_o value: DA increases and DT decreases it, which correlates with the observed blue-shift [4] and red-shift [9], respectively, of the absorption band with the maximum at the wavelength 380 nm, which authors of [4, 9] related to the allowed dipole transition $h_g, g_g \rightarrow t_{1g}$. On the other hand, the deposition of metal nanoparticles (both Ag and Au) onto the C_{60} films, functionalized with 1,8-diaminooctane or octane-1,8-dithiol, respectively, changes their optical parameters in a similar manner, i.e. decreases E_g , E_o and E_U . The latter fact is an evidence of diminishing the structural disorder in C_{60} films caused by the stable and homogeneous incorporation of metal nanoparticles of ca. 5 nm average diameters ensured with previous chemical modification of C_{60} film.

4. Conclusions

The determined dispersion of optical parameters for thin modified C_{60} films on Si substrate and the detailed analysis of their absorption coefficient (α) spectra near the fundamental absorption edge (by using various coordinate systems for α vs hv dependences) allowed us to distinguish regularities of their change caused by modification in the framework of the one-layer model used for their description:

- The direct band gap (or mobility gap) value ($E_g = 2.34 \pm 0.02$ eV) does not practically change in a consequence of diaminooctane or dithioloctane treatment of C_{60} film with a slight decrease of it after deposition of the metal (Ag, Au) nanoparticles.

- Both DA and DT gas-phase treatments of C_{60} film causing the transformation of pristine C_{60} into different solid phases with covalently cross-linked fullerene molecules change the optical gap value E_o (according to the Tauc model) in a different way: DA increases, and DT decreases E_o ; moreover the Urbach tail parameters E_U are changed in the opposite direction.

- Deposition of the metal (Ag, Au) nanoparticles onto chemically modified C_{60} films decreases all their optical parameters (E_g , E_o , and E_U), which testifies

diminishing the structural disorder in C₆₀ films. So, such modifications of thin C₆₀ fullerene films may be promising for their application in energy conversion and photonic devices.

Acknowledgement

Financial support from the National Autonomous University of Mexico (grant DGAPA IN 103009) and from the National Council of Science and Technology of Mexico (grant CONACYT 56420) is greatly appreciated. V.M.-L. is grateful to DGAPA for a postdoctoral fellowship.

References

1. V. Capozzi, G. Casamassima, G.F. Lorusso, A. Minafra, R. Piccolo, T. Trovato, A. Valentini, Optical characterization of fullerene C₆₀ thin films // *Synthetic Metals*, **77**, p. 3-5 (1996).
2. E. Alvarez-Zauco, H. Sobral, E.V. Basiuk, J.M. Saniger-Blesa, M. Villagran-Muniz, Polymerization of C₆₀ fullerene thin films by UV pulsed laser irradiation // *Appl. Surf. Sci.*, **248**, p. 243-247 (2005).
3. N.L. Dmitruk, O.Yu. Borkovskaya, S.V. Mamykin, D.O. Naumenko, V. Meza-Laguna, E.V. Basiuk (Golovataya-Dzhymbeeva), I. Puente Lee, Optical and photoelectrical studies of gold nanoparticles-decorated C₆₀ films // *Thin Solid Films*, **518**, p. 1737-1743 (2010).
4. V. Meza-Laguna, E.V. Basiuk (Golovataya-Dzhymbeeva), E. Alvarez-Zauco, D. Acosta-Najarro, V.A. Basiuk, Cross-linking of C₆₀ films with 1,8-diaminooctane and further decoration with silver nanoparticles // *J. Nanoscience and Nanotechnology*, **7**, p. 3563-3571 (2007).
5. N.L. Dmitruk, A.V. Korovin, I.B. Mamontova, Efficiency enhancement of surface barrier solar cells due to excitation of surface plasmon polaritons // *Semicond. Sci. Technol.*, **24**, 125011 (7p), doi:10.1088/0268-1242/24/12/125011 (2009).
6. K. Tanabe, Optical radiation efficiencies of metal nanoparticles for optoelectronic applications // *Mater. Lett.*, **61**, No.23-24, p. 4573-4575 (2007).
7. N.L. Dmitruk, O.Yu. Borkovskaya, S.V. Mamykin, D.O. Naumenko, N.I. Berezovska, I.M. Dmitruk, V. Meza-Laguna, E. Alvarez-Zauco, E.V. Basiuk, Fullerene C₆₀-silver nanoparticles hybrid structures: optical and photoelectric characterization // *J. Nanoscience and Nanotechnology*, **8**, No.11, p. 5958-5965 (2008).
8. R. Zanella, E.V. Basiuk, P. Santiago, V.A. Basiuk, E. Mireles, I. Puente Lee, J.M. Saniger, Deposition of gold nanoparticles onto thiol-functionalized multiwalled carbon nanotubes // *J. Phys. Chem. B*, **109** (34), p. 16290-16295 (2005).
9. V. Meza-Laguna, E.V. Basiuk (Golovataya-Dzhymbeeva), E. Alvarez-Zauco, T.Yu. Gromovoy, O. Amelines-Sarria, M. Bassiuk, I. Puente-Lee, V.A. Basiuk, Fullerene C₆₀ films cross-linker with octane-1,8-dithiol: preparation, characterization and the use as template for chemical deposition of gold nanoparticles // *J. Nanoscience and Nanotechnology*, **8** (8), p. 3828-3837 (2008).
10. V.N. Antonyuk, N.L. Dmitruk, M.F. Medvedeva, Optical constants determination for real and electrochemical etched GaAs surfaces by multi-angle-of incidence ellipsometry, in: *Ellipsometry in Science and Technique*. Nauka, Novosibirsk, p. 66-71 (1987), in Russian.
11. N.L. Dmitruk, O.Yu. Borkovskaya, I.B. Mamontova, O.S. Kondratenko, D.O. Naumenko, E.V. Basiuk (Golovataya-Dzhymbeeva), E. Alvarez-Zauco, Optical and electrical characterization of chemically and photopolymerized C₆₀ thin films on silicon substrates // *Thin Solid Films*, **515**, p. 7716-7720 (2007).
12. M.S. Dresselhaus, G. Dresselhaus, A.M. Rao, and P.C. Ekland, Optical properties of C₆₀ and related materials // *Synthetic Metals*, **78** (3), p. 313-325 (1996).
13. T.L. Makarova, Electrical and optical properties of pristine and polymerized fullerenes. Review // *Fizika tekhnika poluprovodnikov*, **35** (3) p. 257-293 (2001), in Russian.
14. G.D. Cody, The optical absorption edge of α -Si:H, in: *Semiconductors and Semimetals*, edited by J.I. Pankove, Vol. 21, Part B, p. 11-79. Academic, New York, 1984.
15. Tamihiro Gotoh, Shichi Nonomura, Hideki Watanabe, and Shoji Nitta, Temperature dependence of optical absorption edge in C₆₀ thin films // *Phys. Rev. B.*, **58**(15), 10060-10063 (1998).
16. R.W. Lof, M.A. van Veenendaal, B. Koopmans, H.T. Jonkman, and G.A. Sawatzky, Band gap, excitons, and Coulomb interaction in solid C₆₀ // *Phys. Rev. Lett.*, **68** (26), p. 3924-3927 (1992).
17. V.I. Srdanov, C.H. Lee, N.S. Sariciftci, Spectral and photocarrier dynamics in thin films of pristine and alkali-doped C₆₀ // *Thin Solid Films*, **257**, p. 233-243 (1995).
18. S. Kazdoui, R. Ross, and N. Minami, Intermolecular charge-transfer excitation in C₆₀ films: evidence from luminescence and photoconductivity // *Phys. Rev. B*, **52** (16), p. R11665-R11668 (1995).
19. D. Faïman, S. Goren, E.A. Katz, M. Koltun, N. Melnik, A. Shames, S. Shtuina, Structure and optical properties of C₆₀ thin films // *Thin Solid Films*, **295**, p. 283-286 (1997).
20. T. Makarova, I. Zakharova, Analysis of spectral feature of the optical constants of fullerene and halogen-fullerene films near the absorption edge // *Phys. of Sol. State*, **44**, p. 500-503 (2002).
21. H. Zhang, C. Wu, L. Liang, Y. Chen, Y. He, Y. Zhu, N. Ke, J.B. Xu, S.P. Wong, A. Wei, S. Peng, Structural, morphological and optical properties of C₆₀ cluster thin films produced by thermal evaporation under argon gas // *J. Phys.: Condens. Matter*, **13**, p. 2883-2889 (2001).